EUROPEAN COMMISSION

Community research

FIRST-Nuclides

(Contract Number:295722)

DELIVERABLE (D-N°:5.1)
State of the art report

Author(s): **KIT/AMPHOS21**

Reporting period: e.g. 01/01/2012 – 30/06/2013

Date of issue of this report: **30/06/2012**

Start date of project : **01/01/2012** Duration : 36 Months

Project co-funded by the European Commission under the Seventh Euratom Framework Programme for Nuclear Research &Training Activities (2007-2011)		
Dissemination Level		
PU	Public	X
RE	Restricted to a group specified by the partners of the [FIRST-Nuclides] project	
CO	Confidential, only for partners of the [FIRST-Nuclides] project	

FIRST Nuclides

EURATOM

DISTRIBUTION LIST

Name	Number of copies	Comments
Mr. Christophe Davies (European Commission)	One electronic copy submitted via participant portal	
All consortium members and European Commission	One electronic copy available on the FIRST-Nuclides webportal	

TABLE OF CONTENTS

LIST OF FIGURES

LIST OF TABLES

The 7th Framework Pogramme Collaborative Project FIRST-Nuclides: State-of-the-Art and Rationale for Experimental Investigation

Bernhard Kienzler[+], Volker Metz[+],
Ernesto González-Robles Corrales[+], Vanessa Montoya*, Alba Valls* Lara Duro*
[+]Karlsruhe Institute of Technology (KIT), Institut für Nukleare Entsorgung (INE), Karlsruhe, Germany
*Amphos 21 Consulting S.L., Barcelona, Spain

ABSTRACT

The paper presents the State-of-the-Art with respect to the fast / instant release of safety relevant radionuclides from spent nuclear fuel. In the first part of the report basic information is described, such as the characterization of nuclear fuel, irradiation and temperature induced processes in UO_2 during its use in reactors, and disposal concepts for spent nuclear fuel in different countries. Secondly, the State-of-the-Art on fast release is documented by a summary of results obtained from more than 100 published experiments using different samples, experimental techniques, and duration of the experiments. All authors refer to a definition of the fast / instant release as a fraction of the inventory of radionuclides that may be rapidly released from the fuel and fuel assembly materials at the time of canister breaching. In the context of safety analysis, the time of mobilization of this fraction can be considered as an instantaneous release of some radionuclides at the containment failure time. The State-of-the-Art will be updated regularly according to the results obtained in the 7th Framework Pogramme Collaborative Project FIRST-Nuclides.

INTRODUCTION

According to the 7th Framework Pogramme Topic Fission-2011-1.1.1 "research activities in support of implementation of geological disposal", the Collaborative Project (CP) Fast / Instant Release of Safety Relevant Radionuclides from Spent Nuclear Fuel (FIRST-Nuclides) was applied for. The CP started in January 2012 and has a duration of 36 month. The objectives of the project are in line with the Vision Report and the Strategic Research Agenda (SRA) of the "Implementing Geological Disposal – Technology Platform (IGD-TP)". Six experimental facilities having specialized installations and equipment for work with highly radioactive materials and four organizations having specific knowledge enter into an Inter-European collaboration. The experimental facilities will perform studies using high burn-up spent nuclear fuels in combination with advanced analytical methods.
The fast / instant release of radionuclides from spent nuclear fuel was investigated in a series of previous European projects (such as SFS [1, 2], NF-Pro [3], MICADO [4]). Furthermore, mainly French research programs investigated and quantified the rapid release [5-7]. However, several important issues are still open.

For example, in the MICADO project following missing information was described:

- Understanding of the distribution of FGR for more realistic relationships between FGR and release of various fission products.
- Relationships between the FGR and iodine release for LWR fuel.
- Quantification and modelling of long-term retention of fission products on grain boundaries.
- Quantification of the IRF for high burn-up fuel.
- Chemical speciation of the relevant elements especially chemical form of ^{14}C.

Moreover, in a recent publication by L. Johnson et al. [8], new data on the release of ^{137}Cs and ^{129}I from high burn-up fuel (58 to 75 MWd/kgU UOX/MOX) for ~100 days was provided and the following conclusions and main inputs can be extracted from this work:

- Ratio of fractional release to FGR to ^{137}Cs was in the range of the previous works (3:1).
- ^{129}I release was in the order of FGR. But more experimental data are needed.
- Increased power ratings resulted in higher releases of FG, Cs and I.
- Importance of power history of fuel rods was mentioned.
- Contribution of the rim region (FG and ^{137}Cs / ^{129}I accumulation) is unclear.
- Contribution of grain boundary release is unclear.
- ^{79}Se was found below the detection limit of ICP-MS methods indicating no preferential release.
- Fuel sample preparation had significant impact on the results: fragments resulted in higher releases.
- Presence of cladding lead to an underestimation of the rapid release fraction.

The project FIRST-Nuclide will respond to these open questions. The present contribution will report the present state-of-the-art and demonstrate the rationale for these investigations based on expensive experiments using irradiated nuclear fuels in hot cell facilities and application of sophisticated analytical methods and modelling tools.
Karlsruher Institut fuer Technologie (KIT) DE, Amphos 21 Consulting S.L. (AMPHOS21) ES, JOINT RESEARCH CENTRE – INSTITUTE FOR TRANSURANIUM ELEMENTS (JRC-ITU) EC, FORSCHUNGSZENTRUM JUELICH GMBH (JÜLICH) DE, PAUL SCHERRER INSTITUT (PSI) CH, Studiecentrum voor Kernenergie (SCK•CEN) BE, CENTRE NATIONAL DE LA RECHERCHE SCIENTIFIQUE (CNRS) FR, FUNDACIO CTM CENTRE TECNOLOGIC (CTM) ES, Magyar Tudományos Akadémia Energiatudományi Kutatóközpont (MTA EK) HU, STUDSVIK NUCLEAR AB (STUDSVIK) SE. Associated groups contributing also to FIRST-Nuclides are Commissariat à l'energie atomique et aux energies alternatives (CEA) FR, Los Alamos National Laboratory (LANL) USA, Sandia National Laboratory (SNL) USA, National Decommissioning Authority (NDA) UK, National Nuclear Laboratory (NNL) UK, Posiva Oy FI, Teollisuuden Voima Oy (TVO) FI. Due to the French strategy for dealing with spent fuel, CEA hot-lab facilities are not contributing as a beneficiary to the project.

DESCRIPTION OF THE FUEL

The spent nuclear fuel to be considered in the CP FIRST-Nuclides consists of UO_2 fuel. MOX fuel is presently not in the scope of the project. The burn-up covers the range of some 60 GWd/tHM which is representative for present PWRs and BWRS. However, it is hard to define an average burn-up of the fuel, because of the different enrichments and Gd_2O_3 content in fuel rods and the variation of the neutron flux in the upper and lower part of a fuel rod. For this reason different fuels and burn-ups in the experimental program will be used.

UO_2 pellet

Presently, UO_2 is produced from UO_2/U_3O_8 or Ammonium di-Uranate (ADU) powders which are compacted together with sintering aids (initial density 4.5-5 g cm^{-3}) (see Fig. 1). The sintering is performed at ~1700 °C for 2 to 8 hours and grains are formed. The grain size can be adjusted by the sinter process and by additives to the powders such as Cr_2O_3. The grain size influences both the mechanical properties and the FGR of the fuel. Bigger grains show a lower FGR. Additives produce a coating onto the outer surfaces of the grains which reduces the FGR further. However, it is not clear to which extend such additives are in use. Additives up to 50000 ppm of metal oxides can form oxygen defects which can incorporate fission gases. During the sinter process, remaining U(VI) is reduced. Present UO_2 fuels have grain sizes of 10-20 µm, a density of 10.0 to 10.8 g cm^{-3} and the pore sizes are in the range from 5 to 80 µm.

Fig. 1 From powder to pellet: Grain Size: UO2: ∅ 20 µm, Pellet dimensions: PWR 17×17: ∅ 8.17 (AREVA), L 9.8 mm, BWR 10×10: ∅ 8.87 (Atrium 10XP), L: 10.5 mm

Enrichment and possible burn-up

In the early stages of LWR operation, various failure mechanisms of the fuel were experienced. As the cause and effect of these failure mechanisms came to be understood, changes were made in the fuel design, fabrication processes and in-reactor operating procedures that led to improved fuel reliability higher availability, longer operating cycles with shorter and less frequent refuelling outages, steadily increasing burn-up levels and lower

fuel cycle costs. Continuously, the specifications and operating condition for fuel designs increased to meet power plant up-rate and higher burn-ups to achieve better fuel cycle economy. New cladding and structural materials with high corrosion resistance combined with evolutionary fuel assembly design enhancements have introduced to attain higher thermal margins.

In 2003 the OECD/NEA Nuclear Science Committee initiated an Expert Group on Very High Burn-ups in LWRs, which was charged with the single task of delivering a state-of-the-art report on high burn-ups in LWRs. By this group, very high discharge burn-ups are defined as region average burn-ups from 60-100 GWd/t. The 60-100 GWd/t range took the analysis largely beyond the range of current LWR experience (although there is some experience of experimental test rods having been taken into this burn-up range) and looked very much to the future of LWRs. The report covered only conventional LWR fuel assembly designs, which conform to the assembly geometries used in present LWRs and that use conventional oxide fuels [9]. Fig. 2 shows the initial enrichment versus the average discharge burn-up.

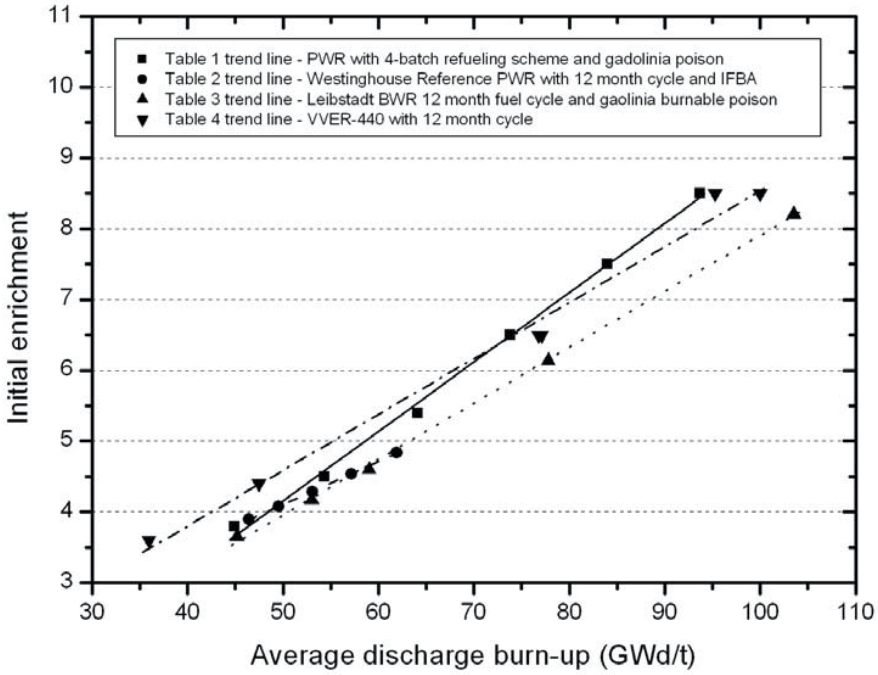

Fig. 2 Initial enrichment versus average discharge burn-up [9]

The initial enrichment relation in Fig. 2 indicates that the maximum average discharge burn-up achievable within the 5.0 wt.% fabrication limit is a little over 60 GWd/t. This figure may be slightly pessimistic, because of the gadolinia residual absorption penalty and because a five- or six-batch scheme or higher (instead of 4 cycles) are known to yield slightly higher average discharge burn-ups for the same initial enrichment.

In BWR KKL, the fuel pellet enrichment varies between 4.46 and 3.71% ^{235}U and density of 10.50 and 10.53 g cm^{-3} respectively. The average grain size is 10–11 µm [10]. In PWR KKG Gösgen, the initial enrichment in UO_2 fuel rods is 4.5 -5.0 % ^{235}U, presently (KKG Broschure 2010). In the PWR GKN II, the enrichment is 4.4 wt.% for fresh UO_2 fuel and 4.6 wt.% for UO_2 from reprocessing.

Fuel Rods

The LWR Fuel Element, both for PWR and BWR, consists of a quadratic arrangement of fuel and control rods. A fuel rod itself consists of a gas-tight zircaloy/M5 cladding and end caps on both ends. At the bottom is a supporting sleeve. Above, an insulating pellet of Al_2O_3 separates the supporting sleeve from the uranium dioxide pellets. The UO_2 pellets are stacked up to the heights of the reactive zone of the reactor. To the top of the fuel rod, again an Al_2O_3 insulating pellet separates the UO_2 pellets from the fission gas plenum, which contains a pressure spring. The spring keeps the pellets in place while reserving some space inside the rod for volume expansion as the pellets become deformed due to heat and neutron radiation, and because of gaseous fission products formation. The fuel rods are charged by He gas up to 22 bar. At the top and bottom, the rods are fixed by an anchor grid, between top and bottom the rods distance between the rods is fixed by spacers.
The rod material consist of Zy2 partly Fe enhanced for BWRs and of M5, Optimised Zry4, Modified Zry4 or Duplex [11] for PWRs.

Fuel Elements / Assemblies

A fuel element consists of the fuel rod, spacers and control rods. The nuclear fuels to be considered in the CP FIRST-Nuclides are originated from, mainly pressure water reactors (PWR), boiling water reactors (BWR), as well as VVER 440 reactors. An overview of relevant fuel element types is given by [11], where four main reactor types (PWR, VVER, BWR and heavy water) are represented. Illustrations and photographs show the representative designs for most of the manufacturers. AREVA produces PWR fuel elements arranged in a square, holding 14x14-(16+1) 15x15-(20+1) 16x16-(20) 17x17-(24+1) to 18x18-(24) fuel rods, for BWRs the ATRIUM fuel elements have 9x9 and 10x10 designs. A cross cut through a BWR fuel element (OL) is shown in Fig. 3 showing the arrangement of the 2 water rods for improvement of moderation and the 12 gadolinium doped rods [12]. These rods are required for high burn-up, where higher initial enrichment is used. For new fuel elements, a reduction of the power peaking factor and a compensation of the excess reactivity is achieved by the burnable neutron poison Gd. Some fuel elements have radially zoned enrichment distributions which reduce the power peaking factor and optimize the heat transfer.

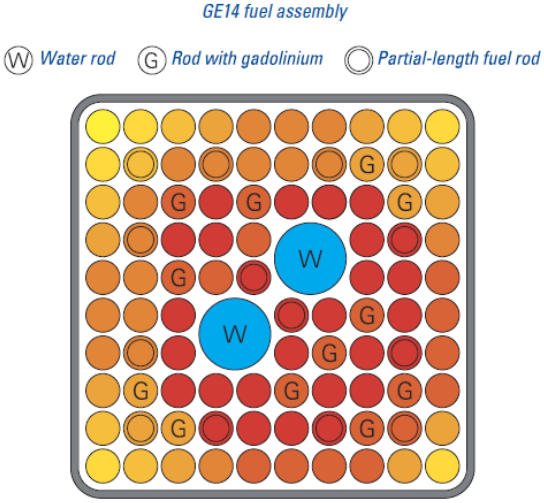

Fig. 3 Arrangement of radially zoned fuel rods, Gd_2O_3 doped rods and water rods in a 10×10 OL1/2 BWR fuel element.

The fuel rods may have many different levels of enrichment zones and burnable absorbers. It is not uncommon to have ten or more different fuel rod designs in a single assembly. It is very important that a fuel rod of a given design be located in its designed position in the assembly [13].

IRRADIATION INDUCED PROCESSES IN UO_2

UO_2 fuel is fabricated by pressing and sintering the powder to a density less than 100% of the theoretical density due to pores in the bulk material. During a burn-up in the range of ~50 GWd/ t HM, about 5.5% of the initial uranium atoms undergo fission (FIMA: Number of fissions per initial metal atom). The fission and fission products cause expansion in the UO_2 crystal structure leading to swelling processes [14].
It was found rather early that the initial porosity reduces the swelling effect. Swelling is a consequence of fission which increases the number of atoms and changes their physical properties. The initial porosity is helpful from this point of view but it introduces secondary effects, for example:

- Influence on all physical properties, e.g. thermal conductivity, creep and strength, and elastic constants.
- Influence moisture and residual gas content of the pellets.
- Potential overcompensation of the swelling during the early reactor irradiation causing rapid shrinkage of small sized pores and a densification of the UO_2.

In the case of the crystal structure, the face-centered cubic UO_2 shows an extended range of composition apart from the exact stoichiometry O/U = 2, so that one may write $UO_{2\pm x}$. The deviation x from the stoichiometric composition affects all physical properties, in particular those which depend on the atomic mobility (e.g. diffusion coefficients), and the oxygen partial pressure or chemical behaviour of the fission products.
The chemical stability of oxides of the fission products in equilibrium with $UO_{2\pm x}$, can be classified into three main groups:

(i) the rare earth elements and Y, Zr, Ba and Sr, whose oxides form either solid solutions with UO_2, or single phase precipitate.

(ii) Mo, Cs and Rb, which are either oxidized or not, depending on the O/U ratio; and elements like Ru, with unstable oxides which form metallic precipitates within the UO_2

The average valence of the fission products is less than 2, therefore the O/U ratio slightly increases during burn-up.

Temperature of the fuel in a reactor

The UO_2 pellets are subject to a high central temperature and a steep radial temperature gradient. Like other ceramic materials, UO_2 shows little thermal shock resistance and behaves in a brittle manner at low temperatures. The vapor pressure increases rapidly with temperature. These properties are responsible for the development of a typical crack pattern in the cool outer part of the pellets and micro-structural changes in the hot inner part of the pellets, up to a complete change in microstructure without melting.

The actual temperature, stresses and behaviour of fuel rods under irradiation are modeled by 2D or 3D codes [15]. For a rough estimation, an analytical equation may be used which relates the linear power to the temperature increase ΔT of a fuel rod.

$$\Delta T = \frac{lin.power}{4\pi \cdot \lambda} \qquad \text{eq. 1}$$

Using eq. 1 following temperatures are obtained for different reactors (The heat conductivity $\lambda_{irrad\ fuel}$ = 2.5 W m^{-1} K^{-1} was used [16]).

Pellet	KKG (PWR)	GKN II (PWR)	KKL (BWR)
∅ [mm]	9.3	8.05	8.5
Lin power [W/cm]	228	167	184
ΔT [K] (eq.1)	725	528	585
$T_{coolant}$ [K]	325	305	263
T_{center} [K]	1050	833	848

During the operation in a power reactor, the temperature causes a radial thermal expansion of the fuel pellets which is partly reversible when cooling.

OPTIMIZATION OF NUCLEAR FUEL (UO_2)

The optimization of the nuclear fuel covers a series of different processes:

- initial enrichment with respect to increased burnup,
- criticality control,
- burnup behaviour, such as swelling
- mechanical and thermal requirements,
- PCI (pellet cladding interactions),
- Minimization of fission gas release by adjusting UO_2 grain sizes, grain pores, and grain coverage.

Most of these optimizations are only described in patents, and they are not openly communicated by the utilities using the fuels. For example, for criticality control, some rods in the fuel elements are doped with Gd. In BWR fuel elements between 1 and 18 rods are doped between 1 and 7 wt.%. In PWR fuel elements between 2 and 12 rods are doped with Gd_2O_3 in the concentration range between 1 and 7 wt. %. The manufacturing process of these binary oxide fuel was published by Assmann [17].
The mechanical and thermal behaviour of the fuel, the UO_2 grain sizes and grain pores are controlled by the sintering process. Various sintering processes have been described (mainly in patents). One example is the NIKUSI low temperature process. The "NIKUSI" process bases on a two step low temperature sintering technique for UO_2 involving sintering at 1100 to 1200°C in CO_2 and later reduction in hydrogen.[18].
Admixtures of various metal oxides control the evolution of mono-disperse grain size during sintering [19-21]. The pore structures and pore sizes of uranium dioxide fuel can also be varied by application of precursor liquids, for example, allylhydridopolycarbosilane (AHPCS) before sintering [22]. Present high burn-up fuel has grain sizes between 20 and 25 µm. This grain sizes give raise to a lower fission gas release (FGR) in comparison to smaller grains.

FGR can also be minimized by covering the UO_2 grains by various ceramic compounds described in some patents.
If and to which extend such specially treated UO_2 is used by the utilities is regarded as companies' secrets.

MODELING TOOLS FOR FUEL PERFORMANCE

The performance of nuclear fuel is affected by the fuel pellet, the properties of uranium oxide, its structure, thermal expansion and thermal conductivity and heat capacity. The properties of the cladding materials have to quarantine compatibility with the UO_2 fuel with respect to thermal properties, linear thermal expansion, thermal conductivity, specific heat capacity and the mechanical properties. These cover the elastic constants and the plastic deformation properties. They account also for irradiation effects, such as irradiation-induced growth and hardening, as well as irradiation-induced creep behaviour. The corrosion and hydrogen pickup of the cladding are also important parameters especially under the high temperature conditions in a reactor.
Modeling tools used by the utilities take into account basic phenomena for in-reactor performance, such as neutronic aspects of fuel, the nuclide evolution, absorbers, heat transfer and thermal characteristics under consideration of the axial heat transport in the coolant, the heat transport in the pellet, the heat transport through the cladding, and the effects of irradiation on gap conductance between the pellets and cladding. The modeling of the mechanical behaviour includes the calculation of strains in the pellet and cladding. Further modeling tools have been developed for studying the fission gas behaviour, for modeling the high burnup structure, pellet-cladding interaction, irradiation-induced stress corrosion cracking and cracking events caused by power ramps. Additionally, a series of codes deal with accidental situations in a reactor core. A comprehensive summary of the relevant basic assumptions and equations are provided by Van Uffelen et al. in a recent Handbook article [23].
A number of different codes are used by the utilities and manufacturers of nuclear fuel. A special issue of the journal "Nuclear Engineering and Design" collected the papers from the IAEA Specialists' Meeting on the Computer Modelling of Nuclear Reactor Fuel Elements, held March 13-17, 1978 at Blackpool, UK (Vol. 56 (1) 1980). Various specialists meetings and workshops have been organized, for example by IAEA [24] and NEA. A recent overview on Fuel Performance Codes was published by Stan [25]. The list of important codes has been provided by Dion Sunderland; Nuclear Science and Technology Interaction Program (NSTIP), ORNL, July 8, 2011). Codes are used for different purposes, e.g. regular fuel performance, but also for "loss-of-coolant accidents (LOCA)". They consider items such as:

- thermal-mechanical behaviour of the fuel (pellet), thermal expansion, creep effects, thermal induced porosity effects and densification, cracking
- fission induced densification and swelling, pore formation
- pellet cladding interactions (PCI),
- chemical properties such as diffusion processes for oxygen and fission products, crystal structure – defects, phase stability of nuclear fuels, especially during transient regimes,

- fission gas release (FGR). A detailed description of effects relevant for FGR is given in the thesis of Peter Blair [26]. Actual FGR code include:
    - Recoil and Knockout
    - Diffusion
    - Diffusion and trapping onto natural defects such as grain boundaries, dislocation lines, closed pores in as fabricated fuel and impurities in the solid. Trapping onto radiation produced defects, such as vacancy cluster, interstitial loops, fission gas bubbles, solid FP precipitates.
    - Gas accumulation in grain boundaries (in grain bubbles, in grain solution between grain boundaries)
    - Sweeping of gas bubbles by grain boundaries
    - Gas break away by gas bubble interaction
    - Bubble migration
- Fabrication imperfections (e.g., MPS): Pellet to cladding mechanical interaction is associated with a defect in the pellet or cladding, such as a missing pellet surface (MPS), which creates excess stress in the cladding. Rapid changes in local power cause pellet expansion, which, in the presence of these stress multipliers, can fail the cladding. The other type of pellet clad interaction is stress corrosion cracking. High power levels promote the release of fission product gases. Iodine in particular is very corrosive to Zircaloy. The presence of iodine near a preexisting cladding imperfection or a stress riser accelerates crack propagation through stress corrosion cracking. PCI can also occur during reactor startup due to rapid changes in core power and unconditioned cladding.

Under the guidance of the Nuclear Science Committee (NSC) of the NEA, Multi-scale Modelling Methods are evaluated (Fig. 4). The expert group aims to provide an overview of the various methods and levels of models used for modelling materials for the nuclear industry (fuels and structural materials). The state of the art includes an overview of the methods but also the possibilities and limits of linking different scales. The report also covers the "Mixed-oxide (MOX) Fuel Performance Benchmark for the Halden Reactor Project MOX Rods [27]. (see http://www.oecd-nea.org/science/wpmm/expert_groups/m3.html).

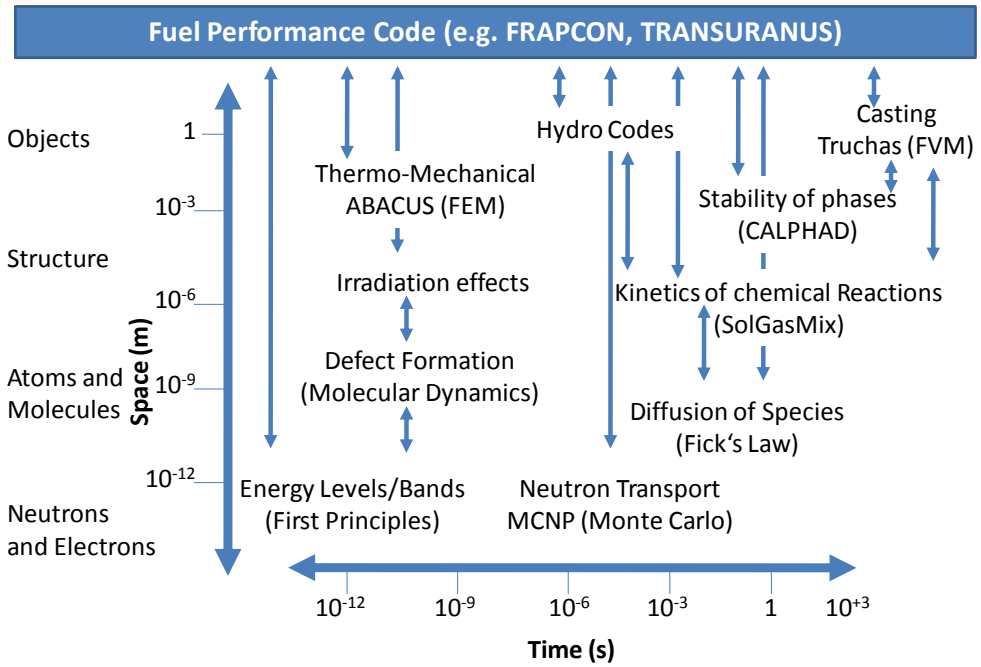

Fig. 4 Space and time scales involved in simulating phenomena relevant for nuclear materials. The methods are shown in parenthesis [28].

Since 2003, annual Materials Modeling and Simulation for Nuclear Fuels (MMSNF) workshops are organized. The goal of the MMSNF workshops is to stimulate research and discussions on modeling and simulations of nuclear fuels, to assist the design of improved fuels and the evaluation of fuel performance. In addition to research focused on existing or improved types of LWR reactors, modeling programs, networks, and links have been created. Examples are organized in EURATOM 7th FP, such as the F-BRIDGE project (Basic Research for Innovative Fuel Design for GEN IV systems (www.f-bridge.eu), the ACTINET network, the EURACT-NMR coordination and support action[1] of to provide access to European nuclear licensed facilities that have recently invested in advanced nuclear magnetic resonance spectrometers.

DISPOSAL OF SPENT NUCLEAR FUEL

Canister concepts

All European disposal concepts for spent nuclear fuel consider thick-walled steel casks having various overpacks or other protecting properties. The different /canister disposal concepts are described in Appendix II.

[1] Nuclear magnetic resonance can provide unique atomic scale structural information in liquids and crystalline and amorphous solids. High resolution instruments operating at KIT-INE (liquids) and JRC-ITU (solids) offer the opportunity to apply this technique to actinide containing materials through the FP7 trans-national access programme EURACT-NMR (www.euract-nmr.eu).

Water contact to the fuel in the casks

Under disposal conditions, one may assume that after a certain period of time water penetrates into the inner steel cask and starts corroding of the steel at the inner steel surfaces causing a hydrogen pressure build-up. Some corrosion mechanisms are shown in Appendix II.

Water access to the spent fuel

Even if a barrier function of the zircaloy cladding of the fuel rods is not considered, the behaviour of this material may affect the instant/fast release of radionuclides from the spent fuel. An irradiated cladding can contain local hydrogen concentrations higher than 1000 ppm. This embrittlement effect of hydrogen in zircaloy is far less at 350°C than that at lower temperatures e.g. 100°C [33]. Under the assumption that water penetrates into the canister, anaerobic corrosion of the steel starts forming hydrogen gas. The gas pressure increases until an equilibrium pressure is achieved which depends on the depth of the repository. At 500 m depth, the maximum pressure is in the range of 5 MPa. This may cause further penetration of H_2 into the zircaloy. Detailed studies of the H_2 effect on the zircaloy embrittlement are available, e.g. [34-36]. Due to the homogeneous distribution of H_2 over the length of the fuel rods, embrittled material zone extends over the complete length of the rods. Therefore, it can be expected that the cladding of the fuel rods will not be damaged by single holes (such as pitting corrosion in stainless steel) but by ruptures, especially at positions where pellet cracking occurred. Maximal cladding hoop stress is located between pellets. Such defects have been investigated in the context of Pellet Cladding Interaction studies [37, 38]. A schematic view is given in Fig. 5.

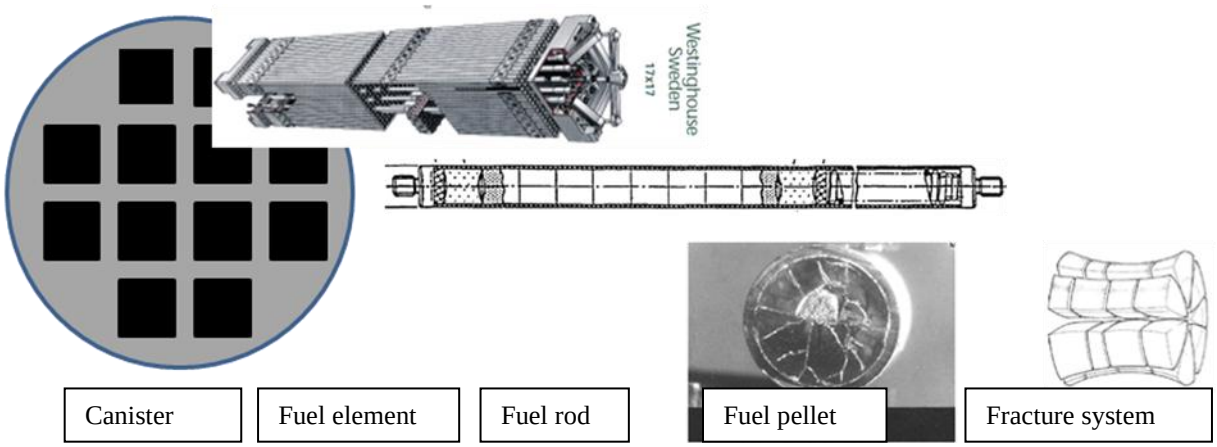

Fig. 5 Pathways for water/solution access to the spent fuel under disposal conditions.

PREVIOUS INVESTIGATIONS ON FAST/INSTANT RELEASE

In the following section, previous investigations, results, and conclusions of the beneficiaries of the CP FIRST-Nuclides are summarized. Most groups relay of Johnson's et al. definition on the fast/instant release [7]: The Spent Nuclear Fuel (SNF) source term in a water- saturated medium is normally described as the combination of two terms:

- A fraction of the inventory of radionuclides that may be rapidly released from the fuel and fuel assembly materials at the time of canister breaching. In the context of safety

analysis, the time of mobilization of this fraction can be considered as an instantaneous release of some radionuclides at the containment failure time.

- A slow long-term contribution corresponding to the dissolution of the uranium oxide matrix, induced by α-radiolytical oxidation processes and impeded by the effect of hydrogen.

In a first approach for the state-of-the-art report, a literature survey is performed covering the published information. In a later step, each beneficiary will provide information on his own investigations, including fuel material, kind of experiments (FGR, dissolution based release), sample sizes, duration of the experiments, solutions composition, pH, pO_2 (Eh), pH_{CO2}, …., and the obtained results.

Tables covering the fast release (leaching) data until 2005 are given by Johnson [2, 7]. In the following, the different leaching experiments with SNF's (UO_2 and MOX) that have been performed during the last 30 years are given. In some cases, the work was not focused in the study of the IRF, however it is possible to calculate it. All the data are listed in Table 1, Table 2 and Table 3. The experiments were carried out using, essentially, four kinds of samples:

- bare fuel: it is a piece of fuel and cladding with a defect.
- pellet: it is used for caldded fuel segment.
- fragments: pieces or portions of fuel without the cladding.
- Powder: amounts of fuel obtained after a complete meachincal procces: decladding, sieving, milling.

- Different publications corresponding to the experiments carried by the USA research can be found; Oversby and Shawn (1987)[39]; Wilson, 1987[40];Wilson and Shawn, 1987[41];Wilson, 1988[42]; Wilson, (1990 a, b)[43, 44]; Wilson and Gray, 1990 [44].

  Two bare fuel specimens were prepared from, HBR (BU of 30 MWd/kgU) and TP (BU of 27 MWd/kgU) PWR SNF's. The tests were conducted in unsealed silica vessels under ambient hot cell air and temperature conditions. The initial weight was 83.10 g for HBR SNF and 27.21 g for TP SNF. The leachant was J-13 water, which composition in mg/L was: Na^+ 50; K^+ 5; Ca^{2+} 15; Mg^{2+} 2;Si 32; F^- 7;$N0_3^-$ 9; $S0_4^{2-}$ 19; $HC0_3^-$ 120; pH 7.2. Two leaching cycles were performed, the Cycle 2 was started the day after Cycle 1 termination. Th experiments were carried at 25 and 85°C.
  The data reported in Table 1 correspond to the sum of the two cycles that means a total leaching time of 425 days for HBR SNF and 376 days for TP SNF.
- Forsyth and Werme, (1992) [45]; Forsyth, (1997) [46]: experiments performed with 20mm long fuel/clad segments from Oskarsham-1 BWR SNF (BU of 42 MWd/KgU), Rignhals-1 BWR SNF (BU between 27.0 and 48.8 MWd/KgU), and from Rignhals-1 PWR SNF (BU of 43 MWd/KgU).

  The specimen, a fuel/clad segment suspended in a spiral of platinum wire, was immersed in 200 ml of leachant in a 250 ml Pyrex flask. All tests were performed at 20-25°C, the ambient temperature of the hot cell, and oxic condition. The leachants used were DIW and GW waters, the composition in mmol/l of the last one is: Na^+ 2.8; K^+ 0.1; Mg^{2+} 0.2; Ca^{2+} 0.45; Si 0.2 HCO_3^- 2.00, Cl^- 2.0; SO_4^{2-} 0.1. The experiments were performed at room temperature.
  The data reported in Table 1 and and Table 2 correspond to a leaching time of 7 days.

- Gray and Wilson, (1995) [47]; Gray [48]: measured the gap and grain boundaries inventories from differents PWR SNF's: ATM-103 (BU of 30MWd/kgU), ATM-104 (BU of 44 MWd/kgU) and ATM-106 (BU of 43 and 46 MWd/kgU), and from BWR SNF's: ATM-105 (BU of 31and 34 MWd/kgU).
  The fuel specimens were prepared from 12 to 25 mm long segments SNF. To measure the gap inventories, the SNF was discharged from the cladding and placed in a glass vessel along with the empty cladding segment. A measured volume (200 to 250 mL) of DIW was added to the vessel and allowed to stand for 1 week at hot cell temperature under ambient atmospher.
  Grain boundary inventory measurements were performed on the SNF specimens after completion of the gap inventory measurements. Following one week exposure to water, the SNF fragments were dried, crushed, and screened using screens with 20 to 30 µm openings, depending on the grain size of the SNF being prepared. The grain-boundary inventory measurements consisted of placing 0.5 g of the screened SNF grains and subgrains in a 50 mL beaker along with 20 mL of 0.1 M HCl. Periodically over 3 h the acid was removed, filtered, and replaced with fresh acid.
  The data reported in Table 1and Table2 were taken from the graphics and as an average of several measures.
- Serrano et al., 1998 [49]: irradiated fuel samples were prepared from pins of two SNF's: UO_2 (BU of 54 MWD/kgU) and MOX (BU of 30MWd/KgU). Sequential batch leaching experiments in DIW at room temperature under ambient atmosphere were performed. On completion of the chosen contact period, the samples were transferred to clean vessels containing fresh leachant. The leaching times encompassed an interval between 24 and 1300 hours. The used vessels were rinsed with 1N HNO_3 for 1h at room temperature. During the tests, the vessels were kept close-tight; after the longest leaching time, no significant loss of leachate from the bottles was observed. The leaching tests with irradiated fuel were performed in a hot cell, at ambient hot cell temperature of 25 ± 2°C.
  The data given in Table 1 and Table 3 correspond to a leaching time of 31 days. The matrix contribution was subtracted.
- Glatz et al., 1999 [50]: Three MOX SNF´s (BU of 12, 20 and 25 MWd/KgU) and three UO_2 SNF´s (one with 30 MWd/KgU and two with 50 MWd/KgU) rodlets, each of them about 6 cm long, were used. Both ends of each sample were closed by means of tight stainless steel end-caps. One UO_2 fuel rod with a burn-up of 50 GWd/tU was provided with two series of defects (in each case, 3 holes of 1 mm diameter each), one series at the top and in contact with vapour and the other at the bottom of the rodlet and in contact with the leaching solution. In all the other samples, the defects were placed in the centre of the rodlet and the autoclave was filled completely with the leaching solution. MOX fuels were fabricated following the MIMAS blend process. The leaching experiments were carried out in autoclaves equipped with Ti-liners using DIW at 100°C under anoxic or reducing conditions.

  The data given in Table 1 and Table 3 correspond to a leaching time of 365 days without the matrix contribution.
- Loida et al., 1999 [51] reported ^{137}Cs the initial release of ^{137}Cs from various spent fuel materials measured in $MgCl_2$-rich and concentrated NaCl solutions at 25, 90, 100, 150 and 200°C. The materials, sample sizes, duration of the experiments, and solutions composition

are summarized in Table 1 and Table 3. These experiments cover mainly fuels of a burn-up between 36 and 50 GWd/t_{HM}. Most of the ^{137}Cs IRF are below or in the range of the pessimistic values compiled by Poinssot and Gras (2009) [52]. A IRF of 3.7% of the total ^{137}Cs was measured in a leaching experiment with a spent nuclear fuel sample from the NPP Biblis (KWB, discharged June 1979; burnup of 36.6 GWd /(t HM)) in concentrated NaCl solution at 200°C. This value is slightly higher than the pessimistic ^{137}Cs IRF estimate for fuel with a burn-up of 41 GWd /(t HM).
The experiments were performed partly at FZK (today KIT) and partly at KWU.

- Quiñones et al., (2006) [53]: three UO_2 PWR SNF's were studied: U-568 (BU of 29.5), B4 (BU of 53.1) and AF-02 (BU of 62.8 Mwd/kgU). Two samples of each specimen were prepared. A whole disc of approximately 2 mm thick, cut from the rods, together with the cladding were obtained. The weight of the SNF contained in these discs was about 2 g.
  Static batch leaching experiments were performed in 70 ml volume borosilicate glass vessels. All tests were performed at room temperature, in a hot cell with air atmosphere. The leachant consisted of 50 ml of CGW, which composition in mol/kg_{H2O} was: Na^+ $4.09\cdot10^{-4}$; K^+ $1.46\cdot10^{-4}$; Mg^{2+} $2.51\cdot10^{-4}$; Ca^{2+} $2.47\cdot10^{-4}$; Cl^- $2.37\cdot10^{-4}$; Si $4.99\cdot10^{-4}$; SO_4^{2-} $7.19\cdot10^{-5}$; HCO_3^- $1.07\cdot10^{-3}$; F^- $1.05\cdot10^{-5}$; PO_4^{3-} $1.04\cdot10^{-7}$; Al^{3+} $1.85\cdot10^{-7}$; Utotal $2.32\cdot10^{-9}$; pH around 7.0. The leachant was deaerated by purging with inert gas for several hours prior to the start of the leaching. During each contact period, the vessels remained sealed. The leaching experiments were performed by taking aliquots of leachate (1 ml) without replacement from the reaction vessel.
  The data reported in Table 1 were obtained from the graphics and represent average values of repeat measurements, the values referred to Rb are quite high in comparison with the values reported for others authors. The leaching time was 500 days for U-568 SNF, and 600 days for B4 and AF-02 SNF's.
- Roudil et al., (2007) [54], Roudil et al., (2009) [55]: five PWR SNF's, four UOX with a BU of 22, 37, 47 and 60 MWd/kgU; one MOX with a BU of 40 MWd/kgU. Two kinds of sample were used: 20 mm segments with cladding and powder samples with a particle size of 20 – 50 µm, the powder sample were only prepared for the SNF with a BU of 60 MWd/kgU. The experiments were carried out in oxic conditions at room temperature (25°C).
  The gap inventories were determined by static mode leaching experiments in carbonate water (HCO_3^-= 10^{-3} M) with 20 mm clad segments of the five SNF´s. The tests, under air atmosphere, lasted 62 days with solution samples taken at the following intervals: 3, 10, 24 and 62.
  Experiments to determine the inventory at the grain boundaries were carried out only on UOX PWR fuel with a BU of 60 MWd/kgU. Leaching experiments were carried out on SNF powder according to a protocol similar to the one developed and validated by Gray [47].
  SNF fragments were sampled from the center of a clad 35 mm segment previously leached for one week in carbonated water to eliminate the gap inventory. Sampling the fragments at the center of the segment also eliminated the contribution of the rim. Powder samples with a particle size fraction of 20–50 µm were therefore prepared by grinding and sieving in a hot cell. The number of grains in each particle was estimated at about forty.
  Pseudo-dynamic leach tests, under air atmosphere in hot cell, were carried out on 567 mg of powder in 25 mL of carbonated water ($NaHCO_3$ = 10^{-2} M) to prevent any precipitation of uranium used as a matrix alteration tracer. After each cycle the solutions were filtered and analyzed. Fresh water was added to the leaching reactors. Thirty cycles were carried

out, initially of short duration (1–2 h) to avoid any precipitation resulting from leaching of the oxidized UO_{2+x} layer, then longer (24–48 h). When the ratio of the released fractions was equal to 1 it was assumed that the complete inventory at the grain boundaries was leached during the preceding cycles.
Roudil et al., 2009 [55]: studied the IRF coming from fragments and grains from the pellet peripheral zone coupon, near or in contact with the cladding. Th used a PWR SNF´s with a BU of 60 MWd/kgU.
Each fuel segment was first slotted to obtain two cylindrical portions separated from the core and consisting of cladding and peripheral Fuel. The cladding was the separated from the fuel with a mortar and pestle. The resulting framents were then separated on 20 and 50 microns screens. To increase the proportion of small grains, such as those in the rim, the powder used for the leaching experiments was sampled from the particle size fraction below 20 microns. Rim grain size is lower than 20 m but this stainless steel.
The leach tests were carried out on 282 mg of powder in about 25ml of bicabornate water to prevent any precipitation of uranium used as a matrix alteration tracer. After each cycle a solution sample of about 17 mL was removed to avoid carrying away powder, filtered to contact with the fuel powder for the next cycle. Twenty cycles were performed in all. The initial cycles were shorter (lasting only few hours) to avoid uranium precipitation due to leaching of the oxidized UO_{2+x} layer. The subsequent cycles were then maintained for 24 hours each.

- Kim et al., (2007) [56]: measured gap and grain boundaries in three different PWR fuel rods: SFR1 (BU of 39.6 MWd/kgU), SFR2 (BU of 39.6 MWd/kgU), SFR3-a (BU of 45.8 MWd/kgU) and SFR3-b (BU of 65.9 MWd/kgU). The fuel specimens were prepared by cutting the fuels rods to a 2 mm thickness.
  The gap inventory was measured with a SNF pellet without cladding. The SNF and cladding were put into a bottle filled with 100 ml of distilled water and put under the hot cell operation conditions. After a soaking of the SNF and cladding, 5 ml of the solutions were sampled with longer than 7 days of time intervals.
  Two types of SNF powder, sawdust produced during the cutting of fuel rod SFR1 and crushed powder produced by crushing the specimens after the gap inventory experiment, were used for a measurement of the nuclide s inventories in the grain boundaries. In the case of the sawdust, the inventory of the nuclides in the grain boundaries was calculated from the IRF which is the combined inventories of the gap and the grain boundaries. The powder was leached in 50 ml of 0.1M HCl for about 20 minutes and the solution was sampled by filtering it with a 0.2 filter. The solution was replaced with a fresh acid and subsequently sampled.
- Fors, 2009 [57]; Fors et al., 2009 [58]. A commercial UO_2 SNF with a BU of 59.1 MWd/kgU and an average power line of 250KW/m was used.
  A 10 mm long segment was cut from a position of the fuel rod. The segment was core drilled to separate the fuel centre from its peripheral 725 µm thick part. The fuel containing the HBS material was detached from the Zircaloy cladding by use of external stress in a screw clamp. The de-cladded fuel fragments contained about 15 wt.% HBS. The millimetre-sized fragments were stored under dry N_2 atmosphere (<2 vol.% O2) for one year before the start of the corrosion experiment. The leachant contained 10 mM NaCl and 2mM $NaHCO_3$. The pH of the initial solution was 8.1. After the leachant filling, the autoclave was pressurized to 4.1 MPa with hydrogen. This pressure was kept throughout the experiment. The experiment was carried out at ambient hot cell temperature, 23 ± 4°C. The leachate was not stirred.

The results given in table 1 refer to a leaching time of 7 days.

- Johnson et al., 2012 [8]: this publication contains two works performed at Studsvik and Paul Scherrer Institute (PSI).
  Studsvik: Four commercials UO_2 SNF´s were used: Ringhals 3 (PWR, BU of 58.2 MWd/kgU), Ringhals 4 (PWR, BU of 61.4 MWd/kgU, Ringhals 3 (PWR, BU of 66.5 MWd/kgU and North Anna (PWR, BU of 75.4 MWd/kgU).
  Two samples were cut from near the middle of each of the four fuel rods: a fuel corrosion sample, consisting of a 20 mm segment, cut at mid-pellet height, containing one complete and two half pellets. These samples are referred to as closed rod samples. In another set of tests, referred to as open rod samples, adjacent fuel rod segments of 20 mm length were cut from each of the four rods and were weighed. The cladding was carefully sawn on both sides of the segment periphery and force was applied to the halves until the fuel broke away from the cladding. The two cladding halves, together with detached fuel fragments were collected in a glass vessel with glass filter bottom (100–160 lm pores) and weighed again. Then they were leached according to the same procedure as for the closed rod samples. An initial solution sampling 2 h after test start was also carried out for all samples of this test series.
  The samples, kept in position by a platinum wire spiral, were exposed to 200 ml of synthetic Allard groundwater in a Pyrex flask. pH was stable around 8.3 and carbonate remained constant during all the tests. The composition of the Allard water in mM was: 0.45 Ca^{+}, 0.18 Mg^{+}, 0.1 K^{+}, 2.84 Na^{+}, 0.21 Si, 2.01 HCO_3^{-}, 0.1 SO_4^{2-}, 1.97 Cl^{-}, 0.2 F^{-}, 0.001 $PO4^{-}$. The contact periods were 2 h, 7, 21 and 63 days. More information about these experiments can be found in [59].
  PSI: Three commercials SNF´s were used: Leibstadt (BWR, UO_2 BU of 65.3 MWd/kgU) Gösgen (PWR, UO_2 BU of 64 MWd/kgU), Gösgen (PWR, MOX BU of 63 MWd/kgU). The length of the fuel rod segments was selected as 20 mm each (two pellets) for the leach experiments. For the rim samples the inner part of the fuel was removed mechanically by drilling (unintentionally somewhat off-center), leaving an asymmetric ring of fuel bonded to the cladding. One rim sample was left open, whereas a tight-fitting PVC plug was placed through the entire length of the other rim sample. In order to investigate if the fuel surface available for the attack of the leachant has a significant impact on the leach rate, a number of samples were broken into two halves by cutting the cladding on opposite sides.
  Glass columns (total volume approx. 250 ml) with a sealed outlet cock for sampling and an implemented glass filter in order to retain solid particles were used. Approximately 200 ml of buffer solution (28 mM borate buffer, pH 8.5, containing 20 µg/g NaI as iodine carrier) were used per sample for the leaching experiments. As the objective of the measurements was to obtain the rapid release fraction of certain radionuclides, the experiments were performed in air-saturated buffer solutions. After filling the columns with the sample and buffer solution the supernatant air volume was removed through a hole in the piston cylinder which was closed afterwards to avoid additional air intake. Subsamples of 20 ml each were taken after 7, 14, 21, 28 and 56 days, whereas the last sampling of 30 ml per leach solution was performed after 98 days.
- Clarens et al., 2009 [60], González-Robles, 2011 [61], Serrano-Purroy et al., 2012 [62]: Four commercial UO_2 SNF´s were selected: three from PWR with a BU of 48, 52, 60, MWd/kgU and one from a BWR with a BU of 53MWd/kgU. The temperature was (24 ± 6)°C.
  From the SNF´s with a BU of 48 and 60MWd/kgU, three different SNF samples corresponding to the central axial position (labelled CORE), the periphery of the SNF

pellet (labelled OUT) and to an emptied cladding segment with small amounts of SNF attached to the inner wall called CLAD. In order to remove fines attached to the grain surface, the CORE and OUT powder SNF fractions were washed several times with acetone.

Static experiments for powder samples, CORE, OUT and CLAD, were carried out in (50 ± 0.1) mL borosilicate glass test tubes of (150 x 25) mm with thread and a plastic screw cap (Schütt Labortechnik GmbH, Göttingen, Germany). The tubes were placed on a rotating stirrer (nominal speed of 30 rpm) to avoid concentration gradients that could influence the dissolution rate. Static leaching experiments were carried out with two synthetic leaching solutions: bicarbonate (BIC), which composition in mM was: 19 Cl^-; 20 Na^+; 1HCO_3^-, pH 7.4; and Bentonitic Granitic Groundwater (BGW), which composition in mM was: Cl^- 93.9; SO_4^{2-} 45.2; HCO_3^- 0.9; Na^+ 117.9; K^+ 1.1; Ca^{2+} 15.4; Mg^{2+} 17.3; pH of 7.6. The experiments were carried out under oxidising conditions and with about 0.25 g of SNF. [60-62].

Static experiments for pellet samples of the four SNF´s were peformed in a (50 ± 0.1) mL flask and daily shaken during 5 to 10 minutes to avoid the risk of breaking the flask by mechanical shaking [61].

The head space of the gas phase was (3 ± 1) mL, in powder samples, and (10 ± 1) mL in pellet samples. To avoid initial U saturation and secondary phase formation, the solution was completely replenished two times at the beginning of each experiment..

Tab. 1 IRF showing the gap and the grain boundary (gb) contribution, in %, from different PWR SFN's.

SNF Id.	BU (MWd/kgU)	FG (%)	Sample	T (°C)	Solution	Time (days)	Rb gap	Rb gb	Cs gap	Cs gb	Sr gap	Sr gb	I gap	I gb	Mo gap	Mo gb	Tc gap	Tc gb
PWR-HBR[a,b]	31	0.2	bare fuel	25[a]	J-13	425			0.76	0.020		0.025					0.015	0.009
				85[b]	J-13	425							0.284					
PWR-TP[a,b]	27	0.3	bare fuel	25[a]	J-13	376			0.29	0.016		0.012					0.024	0.008
				85[b]	J-13	0.4							0.076					
Ringhals-2[c]	43	1.06	pellet	20-25	GW	7			0.85		0.04							
ATM-103[d]	30	0.25	pellet	25	DIW	7			0.2		0.01							
			powder	25	0.1MHCl	60min				0.48		0.11						
ATM-104[d]	44	1.1	pellet	25	DIW	7			1.2									
			powder	25	0.1MHCl	60min				0.1								
ATM-106[d]	43	7.4	pellet	25	DIW	7			2		0.11		0.1					
			powder	25	0.1MHCl	60min				0.5		0.03		8.5			0.13	
ATM-106[d]	46	11	pellet	25	DIW	7			2.5		0.02		1.2				0.01	
			powder	25	0.1M HCl	60min				1.0		0.13		8.0				0.01
ATM-106[d]	50	18	pellet	25	DIW	7			6.5		0.1		15				0.05	
			powder	25	0.1M HCl	60min				1.0		0.07		7.6				0.12
UO_2[e]	54		powder	25 ± 2	DIW	31						0.37				0.26		

SNF Id.	BU (MWd/kgU)	FG (%)	Sample	T (°C)	Solution	Time (days)	Rb gap	Rb gb	Cs gap	Cs gb	Sr gap	Sr gb	I gap	I gb	Mo gap	Mo gb	Tc gap	Tc gb
UO_2[f]	30		bare fuel	100	DIW	365			0.40		0.013							
UO_2[f]	50		bare fuel	100	DIW	365			1.02		0.013							
UO_2[f]	50		bare fuel	100	DIW	365			0.43		0.008							
AL 121/1[g]	52.3		fragment	90	$MgCl_2$	107			1.92									
AL 141/1[g]	52.3		fragment	150	$MgCl_2$	106			2.44									
A6 (0-2)[g]	36.6		pellet	100	$MgCl_2$	57			1.19									
A2 (0-2)[g]	36.6		pellet	200	$MgCl_2$	46			2.24									
A4 (0-2)[g]	37.4		pellet	200	$MgCl_2$	46			17.58									
AL 24/1[g]	52.3		fragment	100	NaCl	100			1.89									
A5 (0-2)[g]	36.6		pellet	100	NaCl	57			1.50									
A1 (0-2)[g]	36.6		pellet	200	NaCl	59			3.68									
A3 (0-2)[g]	37.4		pellet	200	NaCl	59			22.39									
K13W1-2[g]	50.4		pellet	150	NaCl	63			3.48									
K3W1-2[g]	50.4		pellet	25	NaCl	71			1.63									
K4W1-2[g]	50.4		pellet	25	NaCl	73			1.53									
K9W1-2[g]	50.4		pellet	25	NaCl	73			1.16									
K10W1-2[g]	50.4		pellet	25	NaCl	74			1.58									

SNF Id.	BU (MWd/kgU)	FG (%)	Sample	T (°C)	Solution	Time (days)	Rb gap	Rb gb	Cs gap	Cs gb	Sr gap	Sr gb	I gap	I gb	Mo gap	Mo gb	Tc gap	Tc gb
P W 1-3[g]	50.4			25	NaCl	40			2.85									
F3 W 1-2[g]	50.4		fragment	25	NaCl	76			1.34									
F4 W 1-2[g]	50.4		fragment	25	NaCl	76			1.33									
U-568[h]	29		pellet	25	CGW	500	0.05		0.2		0.06				0.01		0.005	
B4[h]	53		pellet	25	CGW	600	36.8		4.2		0.6				0.2		0.1	
AF-02[h]	63		pellet	25	CGW	600	35		4.3		0.6				0.3		0.05	
UOX[i]	22	0.1	pellet	25	HCO_3^- 10^{-3}M	62			0.27		0.025							
UOX[i]	37	0.2	pellet	25	HCO_3^- 10^{-3}M	62			0.6		0.04							
UOX[i]	47	0.5	pellet	25	HCO_3^- 10^{-3}M	62			2.3		0.15							
UOX[i,j]	60	0.8	pellet[i]	25	HCO_3^- 10^{-3}M	62			1.0		0.03							
			powder[i]	25	HCO_3^- 10^{-2}M	110				0.38		0.18						
			powder (rim)[j]	25	HCO_3^- 10^{-2}M	110				>0.48		>0.028						
SFR1[k]	39.6	0.50	pellet	25	DIW	7			0.25		0.03							
			powder	25	0.1M HCl	20 min				1.3≈2.7		0.3						
SFR2[k]	35.0	0.22	pellet	25	DIW	7			0.65		0.03							
			powder	25	0.1M HCl	20 min				0.20		0.09						
SFR3a[k]	45.8	5.0	pellet	25	DIW	7			0.85		0.21							

SNF Id.	BU (MWd/kgU)	FG (%)	Sample	T (°C)	Solution	Time (days)	Rb gap	Rb gb	Cs gap	Cs gb	Sr gap	Sr gb	I gap	I gb	Mo gap	Mo gb	Tc gap	Tc gb
			powder	25	0.1M HCl	20 min				0.20		0.06						
SFR3b[k]	65.9	5.0	pellet	25	DIW	7			1.7	0.20	0.21	0.06						
			powder	25	0.1M HCl	20 min												
UO_2[l]	59.1		fragment	23 ± 4	HCO_3^- 2mM	7			3.4									
Ringhals 3[m]	58.2	0.94	closed	20 ± 2	Allard	90			1.46				0.007					
			open	20 ± 2	Allard	90			1.78				2.29					
Ringhals 3[m]	61.4	2.3	closed	20 ± 2	Allard	90			0.99				0.42					
			open	20 ± 2	Allard	90			1.30				2.16					
Ringhals 4[m]	66.5	2.6	closed	20 ± 2	Allard	90			1.33				0.42					
			open	20 ± 2	Allard	90			1.40				2.28					
Ringhals 3[m]	75.4	5.0	closed	20 ± 2	Allard	98			0.50				2.40					
			open	20 ± 2	Allard	98			2.41				5.23					
Gösgen[m]	64	20.6	closed	25	20mM borate	98			4.12				9.13					
			open	25	20mM borate	98			3.54				4.50					
48BU[n,o]	48		pellet[n]	24 ± 6	HCO_3^- 1mM	10	1.59		6.25		0.05				0.05		0.005	
			powder[n]	24 ± 6	HCO_3^- 1mM	10		4.14[i]		6.06[i]		1.64[i]				1.02[i]		0.10[i]
			powder[n]	24 ± 6	HCO_3^- 1mM	10		1.31[j]		4.45[j]		0.44[j]				0.04[j]		0.002[j]

SNF Id.	BU (MWd/kgU)	FG (%)	Sample	T (°C)	Solution	Time (days)	Rb gap	Rb gb	Cs gap	Cs gb	Sr gap	Sr gb	I gap	I gb	Mo gap	Mo gb	Tc gap	Tc gb
			cladding[o]	24 ± 6	HCO_3^- 1mM	21		0.01		0.001						0.009		
			powder[n]	24 ± 6	BGW	10		2.91		5.23		1.26				1.06		0.09
			powder[n]	24 ± 6	BGW	10		0.37		4.24		0.31				0.01		0.01
			cladding[o]	24 ± 6	BGW	21		0.012		0.005						0.01		
52BU[n]	52		pellet	24 ± 6	HCO_3^- 1mM	10	0.85		3.20		0.08				0.03		0.01	
60BU[n,o,p]	60	15	pellet[n]	24 ± 6	HCO_3^- 1mM	10	0.34		3.20		0.12				0.008		0.007	
			powder[n,p]	24 ± 6	HCO_3^- 1mM	10		1.98[i]		2.45[i]		1.96[i]				0.93[i]		0.31[i]
			powder[n,p]	24 ± 6	HCO_3^- 1mM	10		2.88[j]		3.59[j]		1.52[j]				0.32[j]		0.10[j]
			cladding[o]	24 ± 6	HCO_3^- 1mM	21		0.007		0.38		0.008				0.41		
			powder[n,p]	24 ± 6	BGW	10		2.48		2.15		1.98				1.11		0.40
			powder[n,p]	24 ± 6	BGW	10		2.56		4.26		1.89				0.51		0.03
			cladding[o]	24 ± 6	BGW	21		1.4		1.2		0.32				0.74		0.018

[a][39]; [42]
[b][41]; [44]
[c][45];[46]
[d][47]
[e][49]
[f][50]
[g][51]
[h][53]
[i][54]
[j][55]

[k][56]
[l][57];[58]
[m][8]
[n][61]
[o][60]
[p][62]

Tab. 2 IRF (%) showing the gap and the grain boundary (gb) contribution from different BWR UO2 SFN's.

Fuel Id.	BU (MWd/kg)	FG	Sample	T (°C)	Solution	Time (days)	Rb gap	Rb gb	Cs gap	Cs gb	Sr gap	Sr gb	I gap	I gb	Mo gap	Mo gb	Tc gap	Tc gb
Ringhals-1[a]	27		pellet	20-25	GW	7	0.07		0.2		0.006				0.006		0.005	
Ringhals-1[a]	30.1		pellet	20-25	GW	7	0.08		0.3		0.005				0.006		0.005	
Ringhals-1[a]	32.7		pellet	20-25	GW	7	0.07		0.33		0.008				0.004		0.003	
Ringhals-1[a]	34.9		pellet	20-25	GW	7	0.12		0.5		0.012				0.005		0.004	
Ringhals-1[a]	40.1		pellet	20-25	GW	7	0.16		0.70		0.002				0.001		0.001	
Oskarsham-1[a]	42	0.7	pellet	20-25	DIW	7			0.85		0.004							
Ringhals-1[a]	42.7		pellet	20-25	DIW	7	0.13		0.60		0.002				0.001		0.002	
Ringhals-1[a]	43.8		pellet	20-25	GW	7												
Ringhals-1[a]	45.8		pellet	20-25	GW	7	0.16		0.65		0.007				0.01		0.001	
Ringhals-1[a]	46.5		pellet	20-25	GW	7	0.09		0.51		0.007				0.005		0.008	
Ringhals-1[a]	47		pellet	20-25	GW	7	0.09		0.42		0.005				0.01		0.008	
Ringhals-1[a]	48.1		pellet	20-25	GW	7	0.07		0.34		0.003				0.006		0.007	
Ringhals-1[a]	48.8		pellet	20-25	GW	7	0.03								0.008		0.006	
ATM-105[b]	31	0.59	pellet	25	DIW	7			0.3									
			powder	25	0.1MHCl	60min				0.1		0.08						0.06
ATM-105[b]	34	7.9	pellet	25	DIW	7			1.5		0.0005						0.0005	

			powder	25	0.1MHCl	60min				1.0		0.04						0.06
53BU[c]	53		pellet		1mM HCO_3^-	10	0.06		0.35		0.02				0.004		0.001	
Leibstadt[d]	65.3	3.69	closed	25	20mM borate				1.09									
			open	25	20mM borate				1.38									

[a][45];[46]
[b][47]
[c][61]
[d][8]

Tab. 3 IRF (%) showing the gap and the grain boundary (gb) contribution from different MOX SFN's.

SNF Id.	BU (MWd/kg)	FG (%)	Sample	Solution	T (°C)	Time (days)	Rb gap	Rb gb	Cs gap	Cs gb	Sr gap	Sr gb	I gap	I gb	Mo gap	Mo gb	Tc gap	Tc gb
MOX[a]	30		powder	25 ± 2	DIW	31						0.19				0.02		
MOX[b]	12		bare fuel	100	DIW	365			12.9		0.035							
MOX[b]	20		bare fuel	100	DIW	365			16.5		0.042							
MOX[b]	25		bare fuel	100	DIW	365			14.7		0.042							
AL 29/1[c]			fragment	100	$MgCl_2$	100			3.08									
MOX[d]	47.5	7	pellet	25	HCO_3 10^{-3}M	62			3.2		0.25							
Gösgen[e]	63	26.7	closed	20mM borate		98			4.12				9.13					
			open	20mM borate		98			3.54				4.98					

[a][49]
[b][50]
[c][51]
[d][54]
[e][8]

The content of the tables **Tab. 1** and **Tab. 2** are visualized in the following figures. All data are taken into account, independent on experimental conditions such as sample preparation, aqueous phase, and the use of pellets, fragments or powders, etc.

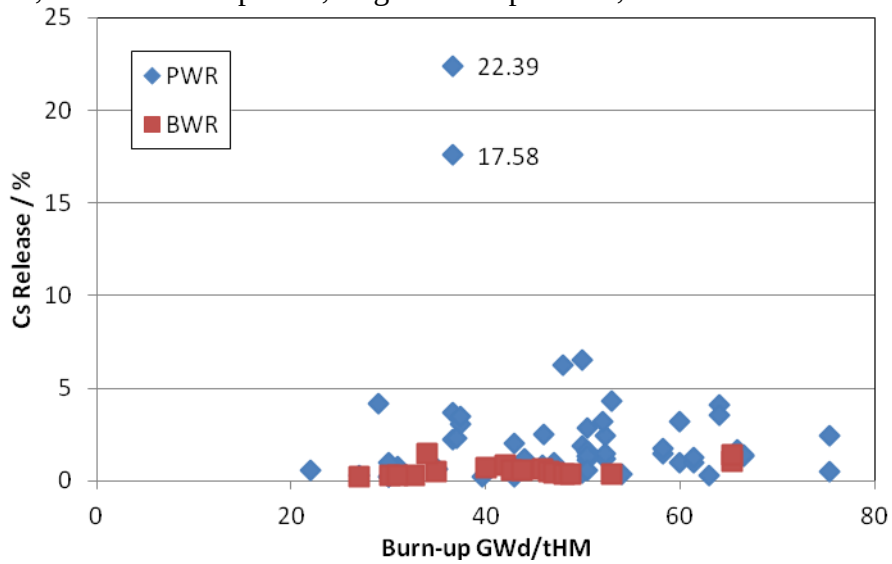

Fig. 6 Fast Cs release as function of the burn-up.

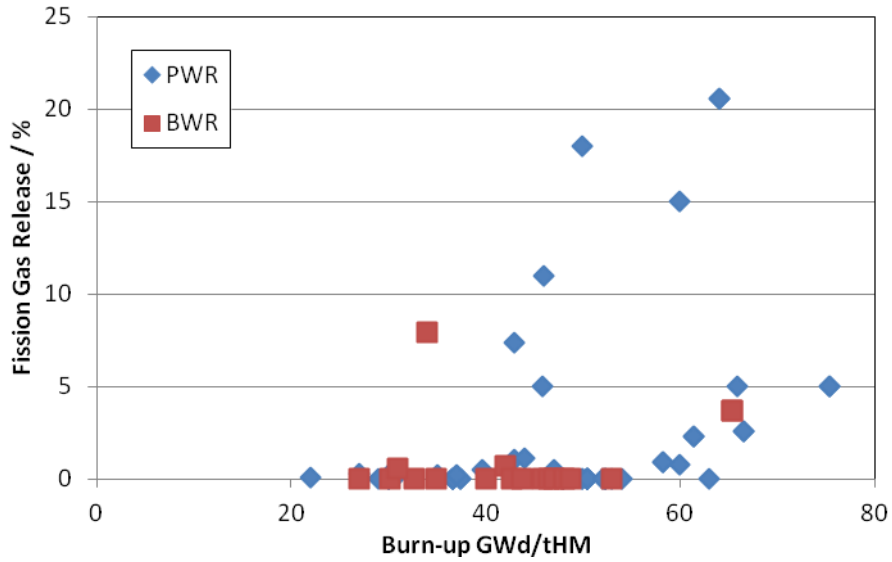

Fig. 7 Fission gas release as function of the burn-up.

Fig. 6 shows the Cs release and Fig. 7 the fission gas release as function of the burn-up for fuel from PWR and BWR. FRG or Cs release of zero means that these data are not given in the related publications. Most of the experiments were performed with fuel having a burn-up below 50 GWd/t_{HM}. In almost all cases, the Cs release is below 5%, only two measurements reveals significantly higher values. In total, the data show a big scatter and especially in Fig. 9 some unclear dependencies exist which do not allow drawing further conclusions. There are two branches in the distributions: One rising at 40 GWd/t_{HM}, another at 60 GWd/t_{HM}. However, considering only those measurements, where both FGR and Cs release have been determined, a different picture appears (Fig. 8).

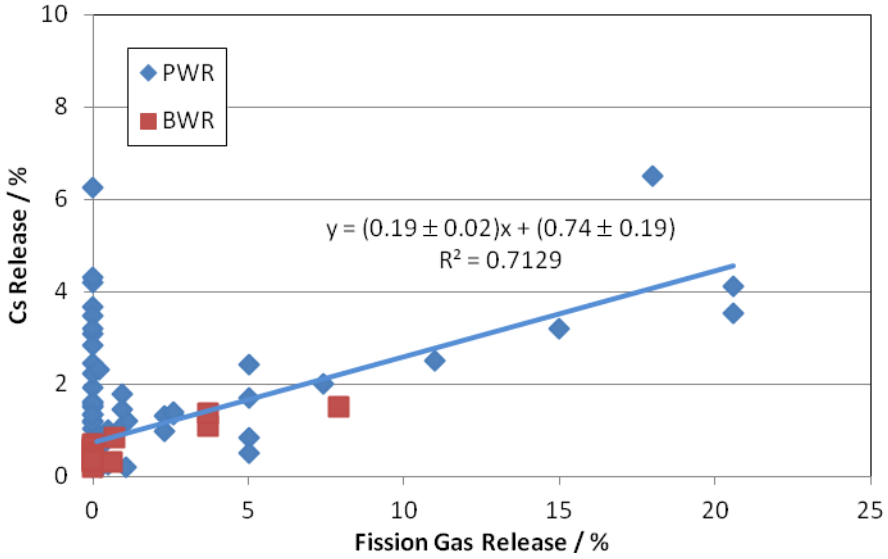

Fig. 8 Cs release as function of the fission gas release.

Neglecting all data points in the preceding tables where only FGR or Cs release is given, a linear correlation between the FGR and the release of Cs in the aqueous phase can be derived:

$$\text{Cs release (\%)} = (0.19 \pm 0.02) \cdot \text{FGR (\%)} + (0.74 \pm 0.19) \qquad \text{eq. 2}$$

It can be concluded, that the complete information on burn-up and other factors are required in order to derive reliable correlations.

SELECTION OF MATERIALS WITHIN FIRST-NUCLIDES

One of the first activities in the CP covers the collection of fuel characterisation data from the beneficiaries. The fuel characterisation covers the type of reactor, its electrical power, types of fuel assemblies, the manufacturers of the fuel and the discharge date of the fuel to be investigated. With respect to the cladding, the characterization covers the material, diameter of rods, material thickness and the initial radial gap width between pellet and gap. The information for the pellet addressed the initial enrichment, geometry, grain size, density and specifics of the production process. The irradiation history covers the burn-up, the irradiation time and the number of cycles as well as the maximum and average linear power rate. Finally information on the fission gas release (FGR) was asked. These information addressed several categories: (i) essential information representing the minimum data and information that should be available for the fuel chosen for the study, (ii) parameters and data which are not directly measured, but are derived from calculations, and (iii) supplemental information referring to characteristics that may be needed depending on the studies to be performed. Spent fuel rods are owned mainly by the reactor operating utilities. KIT, JRC-ITU, JÜLICH, PSI, SCK·CEN, AEKI and Studsvik confirmed the access to the spent fuel material to be used in the project; they have the full rights to perform investigations and to publish the results. A summary of fuel material used during the CP FIRST-Nuclides is provided in Tab. 4 [52]. More information of the characteristics data of the fuel under investigation in CP FIRST-Nuclides can be found in D1.1 of the project (www.firstnuclides.eu).

Tab. 4 Characteristic data of fuel under investigation in CP FIRST-Nuclides.

		PWR	BWR	THTR / VVER
Discharge		1989 -2008	2005 – 2008	
Manufacturer		AREVA	Areva/Westinghouse	
Cladding	**Material**	Zry-4 – M5	Zyr 2	Graphite / Zr1%Nb
	Diameter	9.50 - 10.75 mm	9.84 - 10.2 mm	
	Thickness	0.62 - 0.73 mm		
Pellet	**Enrichment**	3.80 – 4.94 %	3.30 -4.25 %	2.4 -16.8%
	Grain size	5-40 µm	$6 \leq x \leq 25$ µm	20 -80 µm
	Density	10.41 g cm^{-3}	10.52 g cm^{-3}	10.8
	Specifics	standard, NIKUSI production	standard and Al/Cr addition	
Irradiation	**Burn-up**	50.4 – 70.2 GWd/t	48.3 – 57.5 GWd/tU	
	Cycles	2 - 14	5 – 7	
lin. Power	**average**	186 -330 W/cm	160 W/cm	130 – 228 W/cm
FGR		4.9 – 23 %	1.2 – 3.1 %	

Tab. 4 shows that selected materials fit into the range of present high burn-up fuels which need to be disposed of in Europe. Some non-standard materials are included, such as a fuel produced by a low temperature sinter process (NIKUSI), a fuel having Al and Cr additions and a high burn-up fuel kept for 14 cycles in a reactor. The other types of materials cover irradiated and unirradiated TRISO particles and the determination of the activity release from damaged and leaking VVER fuel rods into water environment.

Fuel elements studied in FIRST-Nuclides

BWR fuel from **KKL Leibstadt**, CH and **OL1** and **OL2, Olkiluoto** FIN are used. KKL is a General Electric, Type BWR-6 reactor of 1245 MW_{el} electric power. In this plant, fuel elements type Optima2 (Westinghouse) and Atrium XM (AREVA) are used. In total, KKL needs 648 fuel elements consisting of 96 fuel rods in a 10 × 10 – 4 grid. Each fuel element contains 180 kg uranium. The nuclear power plant units operated by TVO (OL1 and OL2) are identical BWRs of a net electrical output 880 MW_{el} and 860 MW, respectively. The reactors in the OL1 and OL2 power plant units each contain 500 fuel assemblies GE-14 type in a 10 × 10 raster. Each fuel element contains 91–96 fuel rods including 12 rods doped with Gd. The mass of uranium per fuel assembly amounts to 175 kg [12].
PWR fuel from **KKG Gösgen, CH**: KKG uses both UO_2 and MOX. In the CP FIRST-Nuclides, only UO_2 fuel will be considered. KKG needs 177 fuel assemblies, having an overall weight per assembly of 666 kg. Each assembly consists of 205 fuel rods. The initial enrichment is 4.3 % ^{235}U, presently.
VVER fuel: VVER-440 power reactors are a pressurized water reactor using water as coolant and neutron moderator. The **Loviisa** nuclear power plant is operated by Fortum Oy and consists of two VVER 440 units, Loviisa 1 and Loviisa 2 of 488 MW. In the German

Democratic Republic several VVER440 reactors were in operation until 1990. In total, 5050 fuel assemblies of VVER 440 reactors have to be disposed of (vSG). The Hungarian power plants **Paks 1-4** are also of the VVER 440 type. Nuclear fuel for VVER-440 reactors is manufactured and delivered in the form of fuel assemblies. The core of VVER-440 reactor is loaded with working fuel assemblies and control fuel assemblies consisting of the fuel follower of control rod and absorbing extension. Compared to the 4-year fuel cycle, 5-year fuel cycles provide for the additional decrease in natural uranium consumption and number of manufactured, transported and stored fuel assemblies. U-Gd fuel is widely used for this fuel cycle (http://www.elemash.ru/en/production/Products/NFCP/VVER440/).

OBJECTIVES OF FIRST-NUCLIDES IN THE CONTEXT OF PREVIOUS INVESTIGATIONS

The objectives of the CP FIRST-Nuclide are defined in order to respond to open questions raised in the previous projects and publications [1, 2], [3], [4], [5-7] and [8]. The objectives of the CP are directed towards an improved understanding the fast / instant release of radionuclides from high burn-up spent UO_2 fuels from LWRs in geological repositories. The most important is the elaboration of a common definition of "First / Instant Release". The "fast and instant release fraction" was defined within safety analysis of a repository. The long term radionuclide release from spent nuclear fuel under reducing disposal conditions, however, is determined by α-radiolytically induced oxidation processes and impeded by the effect of hydrogen. The definition to be developed should include (i) needs of the project, (ii) delineation to the long-term dissolution processes and (iii) conversion of the short-term experiments and modelling to a "fast and instant release fraction" relevant for long-term safety.

WP 1 includes a discussion of fuel samples and sample preparation for the experiments. The sample sizes fragments or pellets or presence or in absence of cladding have significant impact on the results. It has also to be taken into account, that the fuel rods of several fuel elements including different burn-up or Gd_2O_3 doped material may be disposed in each canister.

The experimental investigations include the release of gaseous and non-gaseous fission products from high burn-up fuel (~ 60 GWd/t_{HM}) and establishing correlations between the fission gas release (FGR) and the release of non-gaseous fission products. A recent study by Johnson et al. [8] demonstrates the importance of the power rate on the FGR. For this reason, it is beneficial for the project to investigate SF from different reactors and different operation strategies, such as number of cycles.

The investigations aim on the reduction of uncertainties with respect to ^{129}I, and ^{14}C, and will provide for improved data for these isotopes. The chemical form of the relevant elements requires also specific investigations, as the migration and retention behaviour depends strongly on their cationic or anionic character.

The experimental work is accompanied by modelling. The prime aim of the modelling is to improve the data base for the fast/instant release fraction of the long-lived fission and activation products from high burn-up spent UO_2 fuel. Modelling will contribute by up-front assessment of the experimental boundary conditions, the coupling of experimental results with model development and the impact of different experimental findings on the refinement of fast/instant release prediction capability. Thereby, up-scaling from the analytical and

modelling micro-scale to the experimental bulk observations and the release on a fuel-rod scale is a key challenge.

REFERENCES

[1] C. Poinssot, C. Ferry, M. Kelm, B. Granbow, A. Martínez, L. Johnson, Z. Andriambolona, J. Bruno, C. Cachoir, J.M. Cavendon, H. Christensen, C. Corbel, C. Jégou, K. Lemmens, A. Loida, P. Lovera, F. Miserque, J. de Pablo, A. Poulesquen, J. Quiñones, V. Rondinella, K. Spahiu, D.H. Wegen, Spent fuel stability under repository conditions – Final report of the European (SFS) project, in, Commissariat à l'énergie atomique (CEA), France, 2005.

[2] L. Johnson, C. Poinssot, C. Ferry, P. Lovera, Estimates of the instant release fraction for UO_2 and MOX fuel at t=0, in: A Report of the Spent Fuel Stability (SFS) Project of the 5th Euratom Framework Program, NAGRA, Wettingen, CH, 2004.

[3] A. Sneyers, Understanding and Physical and Numerical Modelling of the Key Processes in the Near Field and their Coupling for Different Host Rocks and Repository Strategies (NF-PRO), in, SCK•CEN, Brussels, 2008.

[4] B. Grambow, J. Bruno, L. Duro, J. Merino, A. Tamayo, C. Martin, G. Pepin, S. Schumacher, O. Smidt, C. Ferry, C. Jegou, J. Quiñones, E. Iglesias, N.R. Villagra, J.M. Nieto, A. Martínez-Esparza, A. Loida, V. Metz, B. Kienzler, G. Bracke, D. Pellegrini, G. Mathieu, V. Wasselin-Trupin, C. Serres, D. Wegen, M. Jonsson, L. Johnson, K. Lemmens, J. Liu, K. Spahiu, E. Ekeroth, I. Casas, J.d. Pablo, C. Watson, P. Robinson, D. Hodgkinson, Final Report of the Project MICADO: Model uncertainty for the mechanism of dissolution od spent fuel in nuclear waste repository, in, 2010.

[5] C. Ferry, J.P. Piron, A. Poulesquen, C. Poinssot, Radionuclides release from the spent fuel under disposal conditions: Re-Evaluation of the Instant Release Fraction, in: Scientific Basis for Nuclear Waste Management Xxxi, Sheffield, UK, 2007.

[6] P. Lovera, C. Férry, C. Poinssot, L. Johnson, Synthesis report on the relevant diffusion coefficients of fission products and helium in spent nuclear fuel, in, CEA, Direction de L'Énergie Nucléaire, Département de Physico-Chimie, Service d'Études du Comportement des Radionucléides Saclay, 2003.

[7] L. Johnson, C. Ferry, C. Poinssot, P. Lovera, Spent fuel radionuclide source-term model for assessing spent fuel performance in geological disposal. Part I: Assessment of the instant release fraction, Journal of Nuclear Materials, 346 (2005) 56-65.

[8] L. Johnson, I. Günther-Leopold, J.K. Waldis, H.P. Linder, J. Low, D. Cui, E. Ekeroth, K. Spahiu, L.Z. Evins, Rapid aqueous release of fission products from high burn-up LWR fuel: Experimental results and correlations with fission gas release, Journal of Nuclear Materials, 420 (2012) 54-62.

[9] NEA, Very High Burn-ups in Light Water Reactors, OECD/NEA, Paris, F, 2006.

[10] G. LEDERGERBER, S. ABOLHASSANI, M. LIMBÄCK, R.J. LUNDMARK, K.-A. MAGNUSSON, Characterization of High Burnup Fuel for Safety Related Fuel Testing, Journal of Nuclear Science and Technology, 43 (2008) 1006–1014.

[11] Fuel suppliers/designers, Fuel design data, Nuclear Engineering International, 48 (2004) 26-34.

[12] TVO, Nuclear power plant units Olkiluoto 1 and Olkiluoto 2, in, TVO Nuclear Services Oy, Olkiluoto, , FI-27160 EURAJOKI, FINLAND.

[13] J. Deshon, D. Hussey, B. Kendrick, J. McGurk, J. Secker, M. Short, Pressurized Water Reactor Fuel Crud and Corrosion Modeling, Journal of Minerals, Metals and Material Society (JOM), 63 (2011) 64-72.

[14] H. Stehle, H. Assmann, F. Wunderlich, Uranium-Dioxide Properties for Lwr Fuel Rods, Nuclear Engineering and Design, 33 (1975) 230-260.

[15] J.Y.R. Rashid, S.K. Yagnik, R.O. Montgomer, Light Water Reactor Fuel Performance Modeling and Multi-Dimensional Simulation, Journal of Minerals, Metals and Material Society (JOM), 63 (2011) 81-88.

[16] P.G. Lucuta, H. Matzke, I.J. Hastings, A pragmatic approach to modelling thermal conductivity of irradiated UO2 fuel: Review and recommendations, Journal of Nuclear Materials, 232 (1996) 166-180.

[17] H. Assmann, M. Peehs, H. Roepenack, Survey of binary oxide fuel manufacturing and quality control, Journal of Nuclear Materials, 153 (1988) 115-126.

[18] H. Assmann, Advantages of oxidative UO2 sintering process "NIKUSI", in: European Nuclear Society Meeting, Geneva 1986.

[19] G. Gradel, W. Dörr, Method of producing a nuclear fuel sintered body, in, Framatome ANP GmbH (Erlangen, DE), United States, 2004.

[20] W. Dörr, V. Lansmann, FUEL PELLET FOR A NUCLEAR REACTOR AND METHOD FOR THE PRODUCTION THEREOF, in, AREVA NP GmbH (Freyeslebenstrasse 1, 91058 Erlangen, DE), EUROPÄISCHE PATENTSCHRIFT, 2007.

[21] B. Bastide, B. Morel, M. Allibert, Nuclear fuel elements comprising a trap for fission products based on oxide, in, Uranium, Pechiney (Courbevoie, FR), United States, 1993.

[22] J.K. Mccoy, Process for manufacturing enhanced thermal conductivity oxide nuclear fuel and the nuclear fuel, in, AREVA NP Inc. (Lynchburg, VA, US), United States, 2010.

[23] P.V. Uffelen, R.J.M. Konings, C. Vitanza, J. Tulenko, Analysis of Reactor Fuel Rod Behavior, in: D.G. Cacuci (Ed.) Handbook of Nuclear Engineering, Springer Science+Business Media LLC, 2010, pp. 1519-1627.

[24] IAEA, Nuclear fuel behaviour modelling at high burnup and its experimental support, in: Technical Committee, Windermere, United Kingdom, 19-23 June 2000, 2001.

[25] M. Stan, MULTI-SCALE MODELS AND SIMULATIONS OF NUCLEAR FUELS, Nuclear Engineering and Technology, 41 (2009) 39-52.

[26] P. Blair, Modelling of fission gas behaviour in high burnup nuclear fuel, in, École Polytechnique Fédéral, Lausanne, CH, 2008.

[27] T. Tverberg, Mixed-oxide (MOX) Fuel Performance Benchmark: Summary of the Results for the Halden Reactor Project MOX Rods, OECD/NEA, Paris, F, 2007.

[28] M. Stan, Prediction of Nuclear Fuel Materials Properties, in: Transactions, , American Nuclear Society, 2004, pp. 131-133.

[29] R. Graf, W. Filbert, Disposal of Spent Fuel from German Power Plants - Paperwork or Technolgy, in: TopSeal 2006, Olkiluoto, Finland, 17 - 20 September 2006, 2006.

[30] J. Bel, A. Van Cotthem, C. De Bock, Construction, operation and closure of the Belgian repository for long-lived radioactive waste, in: 10th International Conference on Environmental Remediation and Radioactive Waste Management ICEM 2005), Glasgow, UK, 2005.

[31] B. Craeye, G.D. Schutter, H.V. Humbeeck, A.V. Cotthem, Concrete containers for containment of vitrified high-level radioactive waste: The Belgian approach, in: M.G. Alexander, H.-D. Beushausen, F. Dehn, P. Moyo (Eds.) Second International Conference on Concrete Repair, Rehabilitation and Retrofitting (ICCRRR 2008), Cape Town, South Africa, November 2008., Taylor & Francis Group, London, Cape Town, South Africa, November 2008., 2008.

[32] E. Smailos, Influence of welding and heat treatment on corrosion of a high-level waste container material carbon steel in disposal salt brines Corrosion Science, 56 (2000) 1071-1074

[33] P. Rudling, R. Adamson, B. Cox, F. Garzarolli, A. Strasser, High burnup fuel issues, Nuclear Engineering and Technology, 40 (2008).

[34] A.G. Varias, A.R. Massih, Simulation of hydrogen embrittlement in zirconium alloys under stress and temperature gradients, Journal of Nuclear Materials, 279 (2000) 273-285.

[35] J.B. Bai, C. Prioul, D. Francois, Hydride Embrittlement in ZIRCALOY-4 Plate: Part I. Influence of Microstructure on the Hydride Embrittlement in ZIRCALOY-4 at 20 °C and 350 °C, Metallurgical and Materials Transactions A, 25A (1994) 1168.

[36] K.S. Chan, A micromechanical model for predicting hydride embrittlement in nuclear fuel cladding material, Journal of Nuclear Materials, 227 (1996) 220-236.

[37] B. Cox, PELLET CLAD INTERACTION (PCI) FAILURES OF ZIRCONIUM ALLOY FUEL CLADDING - A REVIEW, Journal of Nuclear Materials, 172 (1990) 249-292.

[38] N. Marchal, C. Campos, C. Garnier, Finite element simulation of Pellet-Cladding Interaction (PCI) in nuclear fuel rods, Computational Materials Science, 45 (2009) 821-826.

[39] V.M. Oversby, H.F. Shaw., Spent fuel performance data: An analysis of data relevant to the NNWSI project, in, Lawrence Livermore National Laboratory Report UCID-20926, 1987.

[40] C.N. Wilson, Results from Cycles 1 and 2 of NNWSI Series 2 Spent Fuel Dissolution Tests, in, HEDL-TME 85-22 UC-70, Westinghouse Hanford Company, 1987.

[41] C.N. Wilson, H.F. Shaw, Experimental study of the dissolution of spent fuel at 85 °C in natural groundwater, in: J.D. Bates, W.B. Seefeldt (Eds.) Scientific Basis for Nuclear Waste Management X, Materials Research Society Symposium Proceedings, 1987, pp. 123-130.

[42] C.N. Wilson, Summary of results from the series 2 and series 3 NNWSI bare fuel dissolution test, in: M.J. Apted, R.E. Westerman (Eds.) Scientific Basis for Nuclear Waste Management XI, Materials Research Society Symposium Proceedings, 1988, pp. 473.

[43] C.N. Wilson, Results from NNWSI Series 2 bare fuel dissolution tests. , in: , Pacific Northwest Laboratory Report, PNL-7169, Richland, Washington, USA, 1990.

[44] C.N. Wilson, W.J. Gray, Measurement of soluble nuclide disolution rates from spent fuel, in: M.J. Apted, R.E. Westerman (Eds.) Scientific Basis for Nuclear Waste Management XIII, Materials Research Society Symposium 112, 1990, pp. 473.

[45] R.S. Forsyth, L.O. Werme, Spent fuel corrosion and dissolution, Journal of Nuclear Materials, 190 (1992) 3-19.

[46] R. Forsyth, An Evaluation of Results from the Experimental Programme Performed in the Studsvik Hot Cell Laboratory, in, Svensk Kärnbränslehantering AB, Stockholm, Sweden, 1997, pp. 81.

[47] W.J. Gray, C.N. Wilson, Spent fuel dissolution studies FY 1991 to 1994, in, Pacific Northwest National Laboratory, Richland, Washington, USA, 1995.

[48] W.J. Gray, Inventories of I-129 and Cs-137 in the gaps and grain boundaries of LWR spent fuels, in: D.J. Wronkewiecz, J.H. Lee (Eds.) Scientific Basis for Nuclear Waste Management XXII, Materials Research Society Symposium Proceedings, 1999, pp. 478-494.

[49] J.A. Serrano, V.V. Rondinella, J.P. Glatz, E.H. Toscano, J. Quiñones, P.P. Díaz-Arocas, J. García-Serrano, Comparison of the Leaching Behaviour of Irradiated Fuel, SIMFUEL, and Non-Irradiated UO_2 under Oxic Conditions, Radiochimica Acta, 82 (1998) 33-37.

[50] J.-P. Glatz, J. Giménez, D. Bottomley, Leaching of high burn-up UO2 and MOX fuel rods with pre-set cladding defects, in: WM'99 Conference, 1999.

[51] A. Loida, B. Grambow, M. Kelm, Abgebrannter LWR-Kernbrennstoff: Auslaugverhalten und Freisetzung von Radionukliden. Abschlußbericht BfS-Projekt 9G213532100 (FZK-INE 009/99). in, 1999, pp. 147.

[52] C. Poinssot, J.-M. Gras, Key scientific issues related to the sustainable management of the spent nuclear fuel in the back-end of the fuel cycle, in: N.B.B. Robert J. Finch (Ed.) Scientific Basis for Nuclear Waste Management XXXII, Mat. Res. Soc. Symp. Proc., Boston, USA, 2009.

[53] J. Quiñones, J. Cobos, E. Iglesias, A. Martínez-Esparza, S. Van Winckel, J.P. Glatz, Preliminary approach obtained from Spent Fuel Leaching experiments performed by ITU-ENRESA/CIEMAT, in, CIEMAT, Madrid, Spain, 2006, pp. 27.

[54] D. Roudil, C. Jégou, V. Broudic, B. Muzeau, S. Peuget, X. Deschanels, Gap and grain boundaries inventories from pressurized water reactors spent fuels, Journal of Nuclear Materials, 362 (2007) 411-415.

[55] D. Roudil, Jegou, C., Broudic, V., Tribet, M., Rim instant release radionuclide inventory from French high burnup spent UOX fuel, Materials Research Society Symposium Proceedings 1193 (2009) 627-633.

[56] S.S. Kim, Kang, K. C., Choi, J. W., Seo, H. S., Kwon S. H., Cho. W. J., Measurement of the gap and grain boundary inventories of Cs, Sr and I in domestic used PWR Fuels, Journal of the Korean Radioactive Waste Society, 5 (2007) 79-84.

[57] P. Fors, The effect of dissolved hydrogen on spent nuclear fuel corrosion, in: Department of Chemical and Biological Engineering, Nuclear Chemistry, Chalmers University of Technology, Göteborg, 2009, pp. 132.

[58] P. Fors, P. Carbol, S. Van Winckel, K. Spahiu, Corrosion of high burn-up structured UO_2 fuel in presence of dissolved H_2, Journal of Nuclear Materials, 394 (2009) 1-8.

[59] U. Zwicky, J. Low, E. Ekeroth, Corrosion Studies with High Burnup Light Water Reactor Fuel, in, SKB TR-11-03, Svensk Kärnbränslehantering AB, Stockholm, Sweden, 2011, pp. 84.

[60] F. Clarens, E. González-Robles, F.J. Gimenez, I. Casas, J.d. Pablo, D. Serrano, D.Wegen, J.P. Glatz, A. Martinez-Esparza, Effect of burn-up and high burn-up structure on spent nuclear fuel alteration, in: Publicación técnica 04-2009, Enresa, Madrid, Spain, 2009, pp. 177.

[61] E. González-Robles, Study of Radionuclide Release in commercials UO_2 Spent Nuclear Fuels, in: Departament d'Ingenyeria Quimica, Universitat Politècnica de Catalunya, Barcelona, 2011, pp. 137.

[62] D. Serrano-Purroy, F. Clarens, E. González-Robles, J.P. Glatz, D.H. Wegen, J.d. Pablo, I. Casas, J. Giménez, A. Martínez-Esparza, Instant release fraction and matrix release of high burn-up UO_2 spent nuclear fuel: Effect of high burn-up structure and leaching solution composition, Journal of Nuclear Materials 427 (2012) 249–258.

APPENDIX I: MANUFACTURERS OF UO_2 FUEL AND FUEL ELEMENTS

Nuclear fuel elements are produced for energy production in nuclear power plants. The fuels to be considered in the CP FIRST-Nuclides are uranium oxide fuels having initial enrichments up to 4.3 wt.%. An overview of fuel elements for the different types of reactors was published by [11]. The nuclear fuel used in Europe is mainly produced by subsidiaries of AREVA or Westinghouse.

FBFC (French acronym for Franco-Belgian Fuel Fabrication), a subsidiary of AREVA comprises three sites at Romans (F), Pierrelatte, Tricastin (F), and Dessel (B). The **Romans site** transforms uranium hexafluoride supplied by EURODIF into uranium oxide powder (UO_2). It also fabricates uranium pellets, rods, nozzles, and fuel assemblies for pressurized water reactors (PWRs). FBFC Romans employs 830 persons. The **Pierrelatte site** manufactures support grids for assemblies for PWR fuels and Harmoni™ control clusters. These products are then supplied to the Romans and Dessel plants, which fabricate fuel assemblies. It also produces spacers for MELOX's MOX fuel assemblies. **FBFC International** located in **Dessel**, Belgium, produces fuel assemblies for pressurized water reactors. The plant also fabricates pellets with gadolinium, rods, plugs, and spring packs for fuel assemblies for pressurized water reactors and boiling water reactors. It also assembles the various components for MOX fuel assemblies. At the Tricastin site, EURODIF Production operates the Georges Besse plant performing uranium enrichment by gaseous diffusion. With the new Georges Besse II plant in operation since 2009, AREVA uses the centrifugation technology for enrichment.

Advanced Nuclear Fuels GmbH (ANF) is a full subsidiary of AREVA. Its headquarters are in Lingen (Germany) and its operations are distributed over three sites in Germany. The plant in **Lingen** produces UO_2 powder, as well as pellets, rods, and fuel assemblies for pressurized and boiling water reactors. Since the site's commissioning in 1977, it has produced more than 20,000 fuel elements. Following stages in assembly fabrication are performed at the Lingen plant: uranium hexafluoride (UF_6) is transformed into uranium oxide (UO_2). This oxide is compacted into cylindrical pellets and baked in ultra-high-temperature furnaces. The pellets are then stacked into tubes of around 4 meters in length, called "rods". These are then sealed off at the ends. The zirconium-alloy rod cladding is subjected to rigorous testing. The rods are grouped into assemblies with the appropriate dimensions.

Westinghouse Sweden Nuclear Fuel Factory, situated in Västerås, Sweden. The Fuel Factory manufactures fuel assemblies for PWRs and BWRs, and fuel channels and control rods for BWRs. The factory in Västerås is responsible for the entire chain from research and development to manufacturing of nuclear fuel, as well as for control rods and fuel channels for BWR plants including codes for core surveillance. The present fuel factory has been in operation since 1971, and has continuously been expanded and modernized. The factory produces approximately 400 tons of UO_2 fuel for BWRs and PWRs per year. In the conversion of UF_6 into UO_2 powder, the capacity as well as the plant license is limited to 600 tons UO_2.

British Nuclear Fuels Ltd (BNFL) was the manufacturer fuel elements feeding the British Energy's (BE) AGR reactors as well as BNFL's own Magnox Reactors. Advanced gas-cooled reactor fuel (AGR) comprises 36 stainless steel pins each containing 64 pellets, grouped

together inside a graphite ‘sleeve’ to form a ‘fuel assembly’. BNFL also made fuel for the older Magnox Reactors which comprised a natural uranium metal bar with a magnesium alloy casing. BNFL’s core expertise for fuel manufacture was based on fabrication of the uranium pellets, and the final assembly of the fuel elements. BNFL was finally abolished in 2010.

APPENDIX II: CANISTER/DISPOSAL CONCEPTS

Germany

In Germany, the disposal concept for spent nuclear fuel, the so called "direct disposal of spent fuel" was developed and examined with respect to safety aspects. The reference concept is based on the triple purpose cask POLLUX for transport, storage and final disposal as well as a conditioning technique that separates fuel rods from the structural parts of the fuel assemblies. Another most promising option is called BSK 3-concept. Both concepts are described in the literature [29]. The POLLUX canister consists of a shielding cask with a screwed lid and an inner cask with bolted primary and welded secondary lid. The inner cask consists of fine-grained steel 15 MnNi 6.3, the thickness of the cylindrical wall is 160 mm according the mechanical and shielding requirements. The outer cask provides shielding. Its thickness is 265 mm and it consists of cast iron GGG 40. The weight of the inner cask (including spent fuel is 31 Mg, the weight of the outer cask is 34 Mg. 10 complete fuel elements can be packed into a POLLUX cask. Another possibility is the accommodation of consolidated fuel rods (5.4 tHM). The BSK 3 cask was designed for accommodation of consolidated fuel rods. The capacity of a BSK 3 is designed for three PWR fuel elements or 9 BWR fuel elements. The wall thickness of the BSK 3 is 50 mm.

Sweden

The Swedish/Finish Canister concept bases on an insert of nodular iron (a kind of cast iron) which is inserted into a copper tube (Fig. 9). The copper lids are welded by friction stir welding. The canisters are about 5 metres long and have a diameter of more than one meter. When the canister is filled with 12 spent fuel elements, it weighs between 25 and 27 metric tons. (SKB Brochure “Encapsulation, When, where, how and why?”).

Belgium

In Belgium, the Supercontainer was developed which surrounds the steel cask containing the fuel elements by a thick concrete overpack [30]. The supercontainer is intended for the disposal of (vitrified) high level heat-emitting waste and for the disposal of spent fuel assemblies. In this concept, the spent fuel assemblies are enclosed in a carbon steel overpack of about 30 mm thick. This overpack has to prevent contact of the waste with the water coming from the host formation during the thermal phase of several 1000 years for the spent fuels assemblies. For corrosion protection, the overpack is enveloped by a concrete buffer of about 70 cm thickness. The concrete is surrounded by a stainless steel cylindrical envelope (called liner). The outside radius of the supercontainer for spent fuel assemblies is about 1.9 m, and a length of about 6 m, it’s mass is about 54 tons [31].

Fig. 9 Components of the Swedish canister concept at SKB's Canister Laboratory in Oskarshamn.

In all these concepts, corrosion of the fine-grained steel 15 MnNi 6.3 (Germany), nodular iron (Sweden, Finland) or carbon steel (Belgium) is a prerequisite before groundwater may come into contact with the fuel assemblies. Different corrosion processes may be relevant: The three examples listed above, show general corrosion due to an active corrosion mechanism. Only in the Belgian case, a passivation of the steel may occur. Under the reducing conditions of a deep underground disposal, anaerobic corrosion of the steel takes place forming hydrogen gas. The active corrosion process normally shows a non-uniform thickness reduction, especially if there are gradients in material or mineralogical composition or in the welding material. The degree of non-uniformity in thickness reduction of the actively corroding steels was observed in the range of a factor of 2 in comparison to the general corrosion rate [32]. However, in the case of a heat-affected zone close to the welding, the corrosion rate may increase. For example, **Fig. 10** shows the corrosion of the welding of fine-grained steel in $MgCl_2$ brine at 150°C under γ-irradiation (10 Gy/h).

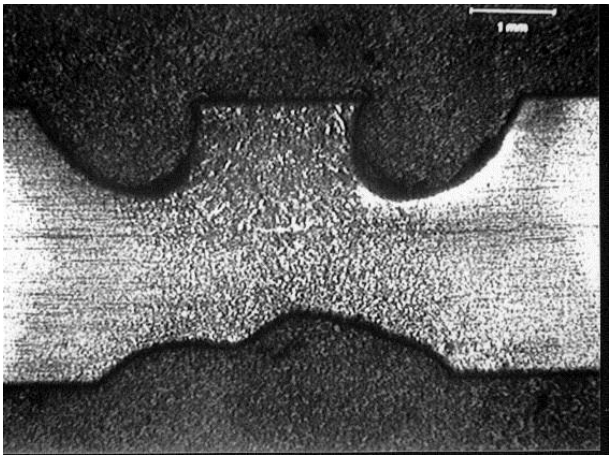

Fine-grained steel welding, untreated

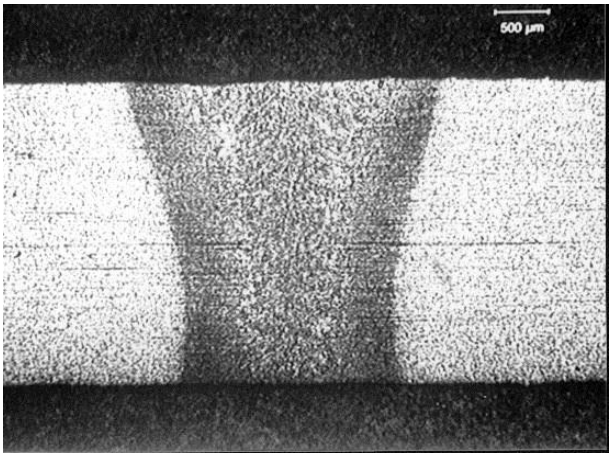

Fine grained steel, heat-treated

Fig. 10 Corrosion of the welding of fine-grained steel 1.0566 (FStE 355) in $MgCl_2$ brine at 150°C under γ-irradiation (10 Gy/h) [32].